Formulation and evaluation of a novel megalomeric microemulsion from tamarind seed xyloglucan-megalosaccharides for improved high-dose quercetin delivery

Weeranuch Lang[1,*], Debashish Mondol[2], Aphichat Trakooncharoenvit[3], Takayoshi Tagami[1], Masayuki Okuyama[1], Tohru Hira[3], Nobuo Sakairi[4], Atsuo Kimura[1,*]

[1]Laboratory of Molecular Enzymology, Research Faculty of Agriculture, Hokkaido University, Sapporo 060-8589, Japan.
[2]Department of Pharmacy, Faculty of Biological Science and Technology, Jashore University of Science and Technology, Jashore 7408, Bangladesh.
[3]Laboratory of Nutritional Biochemistry, Research Faculty of Agriculture, Hokkaido University, Sapporo 060-8589, Japan.
[4]Division of Environmental Materials Science, Faculty of Environmental Earth Science, Hokkaido University, Sapporo 060-0810, Japan.

[*]Corresponding authors.
E-mail addresses: weranuch@abs.agr.hokudai.ac.jp, weranuch24@hotmail.com (W. Lang); kimura@abs.agr.hokudai.ac.jp (A. Kimura).

Abstract

Megalomeric microemulsion is a new term referring to lipid-based formulation using amphiphilic megalosaccharide as a coexcipient. Quercetin is a dose-dependent bioactive compound and has promising therapeutic potential, but its low water solubility and permeability restrict its treatment efficacy. We aimed to formulate high-dose quercetin loaded into colloidal micelles by the self-micro emulsifying system (SMES) in combination with Tween 80, isopropyl myristate, and xyloglucan megalosaccharide (X-MS). X-MS is a moderate-size heterologous saccharide obtained from enzymatic cleavage of tamarind seed xyloglucan. X-MSs with an average degree of polymerization of 16 and 56 were investigated to bearing their surface hydrophobic interaction with a fluorescence probe 6-(*p*-toluidino)-2-naphthalene-6-sulfonate yielded the binding constant values of 127 and 180 M^{-1}, respectively and X-MS itself displayed a slight effect on quercetin binding. However, the implementation of X-MSs toward SMES was highly compatible because X-MS molecules were confined in micellular solutions. Consequently, X-MSs improved the quercetin loading from 1–2 to 12.5–17.7 mg/mL based on the composition ratio, X-MS chain lengths, and X-MS concentrations (0.15–3.0%, w/v) and

stabilized the quercetin-loaded oil-in-water SMES. The optical appearances were transparent yellow containing uniformly fine droplets with diameters of 11–12 nm. In vitro radical scavenging activity tests with 2,2-diphenyl-1-picrylhydrazyl showed that the megalomeric microemulsions improved the half-maximal inhibitory concentration (IC50 = 22–24 μg/mL) over that of the X-MS-free microemulsion. This study provided a new approach of liquid supplementation from commercially unavailable-size xyloglucan to be a promising added-value agent for oral uptake of quercetin.

Keywords: tamarind seed xyloglucan, megalosaccharide, antioxidative flavonoid, cosurfactant, microemulsion formulation, self-emulsifying drug delivery system

1. Introduction

Quercetin is one of the most common plant flavonoids. It exhibits numerous biological and pharmacological effects, such as antioxidant, anticarcinogenic, and antimicrobial activities (Andrés et al., 2013; Dajas, 2012; Johari, Kianmehr, Mustafa, Abubakar, & Zandi, 2012). However, the level of quercetin in blood plasma is less than 1% of the uptake level, primarily due to practical water insolubility (0.17–7.7 μg/mL) and low permeability (Gao et al., 2009). Lipid-based formulations, predominantly the self-emulsifying drug delivery system (SEDDS), are the most promising strategy for drugs with poor bioavailability, as they retain the drug in a predissolved state in the gastrointestinal tract (Wu et al., 2015). SEDDSs emulsify spontaneously to produce fine oil-in-water (O/W) emulsions when introduced into an aqueous phase and the small size of the formed droplet provides a large interfacial surface area for drug absorption. The SEDDS containing an O/W emulsion with a droplet diameter less than 50 nm entrapping the lipophilic drug molecules absolutely with 100% efficacy is known as the self-micro emulsifying system (SMES) (Phan, Le-Vinh, Efiana, & Bernkop-Schnürch, 2019). The SMES is an isotropic dispersion of oil, emulsifier, coemulsifier (organic solvent or other compatible amphiphilic components), and a drug substance. Quercetin-loaded contents in SEDDSs have been documented in the range of 0.067 to 2 mg/mL, while particle sizes within the range of 20–290 nm and some additional treatments, such as heating, ultrasonic exposure, homogenization, and solvent evaporation, may be applied (Liu, Huang, Jhang, Liu, & Wu, 2015; Rogerio et al., 2010; Sermkaew & Plyduang, 2020; Son et al., 2019). For the preparation of a stable SMES formulation, the selection of an appropriate emulsifier and coemulsifier is considered critical since it is a mixture of two immiscible liquids containing nanosized droplets to entrap drug substances (Bai & McClements, 2016). However, to carry a high drug dose, the

required emulsifier/coemulsifier contents must be as high as possible, and those high formulations may lead to toxicity aspects of the corresponding delivery systems (Premathilaka, Rashidinejad, Golding, & Singh, 2022).

Among the numerous notable polymeric emulsifiers/coemulsifiers, polysaccharides have recently become the most preferable since they are highly stable, safe, nontoxic, biodegradable, and naturally available. However, their solution properties of high molecular weight and viscosity are less proficient, as they are not compatible with SMES. Megalomeric microemulsion is a new term designated first time in the present study for lipid formulation-based amphiphilic megalosaccharide (MS) excipients. The terminology of MS, defined by the size composed of 10–100 units of monosaccharide bound together by glycosidic bonds (Thoma & French, 1960), represents the nonsweet middle-size saccharides between oligosaccharides and polysaccharides. Previously, we established a preparation method of homologous glucose-type MS (G-MS) by enzymatic transglucosylation, and G-MS exhibited functional effects in increasing the solubility of quercetin and ethyl red dye and provided a barrier function against paracellular transporters (Shinoki et al., 2013; Lang et al., 2014, 2022a, b; Hara, Kume, Iizuka, Fujimoto, & Kimura, 2017). In the present study, we focused on the preparation of heterologous MSs by the considerably simpler enzymatic hydrolysis of tamarind (*Tamarindus indica* L.) seed xyloglucan. Xyloglucan has versatile industrial and pharmaceutical applications as a neutral thickener, stabilizer, and gelling agent in which the purification method of the seed gum has a great influence on those properties (Crispín-Isidro et al., 2019). The main structure of xyloglucan is a cellulose-like β-(1→4)-linked glucan backbone and branch chains substituted with galactose, xylose, and arabinose (Majee, Avlani, & Biswas, 2016). Accordingly, xyloglucan MS (X-MS) is proposed to aid as a compatible coemulsifier to stabilize quercetin in dissolved form to reach the required therapeutic plasma concentration as well as decrease the toxic quantities conferred by the emulsifier and organic solvents. X-MS was hypothesized to participate in the micelles by taking the place of their branched molecules between the interfacial layer of the head and tail groups of the emulsifier (e.g., Tween 80). The specific hydrophobic force may strongly confine hydrophobic guest molecules into the hydrophobic core and eventually stabilize their conformation.

In our study, X-MSs were prepared by cellulase cleavage into two sizes and characterized for their hydrophobic properties. The interaction of X-MSs in terms of synergistically cooperating with Tween 80 micelles was investigated by fluorescence spectroscopy. Polyethylene glycols (PEGs) with several chain lengths are screened as the coadjutant replacing common traditional solvents, such as dimethyl sulfoxide and methanol.

The quercetin formulation was adjusted by constructing a ternary phase diagram. Two formulations were applied to compare a load of quercetin with the addition of X-MSs and several saccharides. In vitro antioxidant assays with two free radical compounds, 2,2-di(4-tert-octylphenyl)-1-picrylhydrazyl (DPPH) and 2,2'-azino-bis(3-ethylbenzothiazoline-6-sulfonic acid (ABTS), were further examined.

2. Materials and Methods

2.1. Materials. High-purity-grade tamarind seed xyloglucan and quercetin hydrate were purchased from Tokyo Chemical Industry (Tokyo, Japan). PEG 200, 300, 400, and cyclodextrins (CDs) were purchased from Fujifilm Wako Pure Chemical Corporation (Osaka, Japan). PEG 550 and all higher-molecular-weight PEGs and ABTS diammonium salt were obtained from Fluka (Steinheim, Germany). 6-(*p*-Toluidino)-2-naphthalenesulfonic acid sodium salt (TNS) and DPPH were purchased from Sigma–Aldrich (St. Louis, MO, USA). Dextran T 40 was available from Amersham Biosciences (Uppsala, Sweden), and dextran T 3.5 and T 6 were ordered from Pharmacosmos (Holbaek, Denmark). Glycerol was purchased from Hampton Research (Aliso Viejo, CA, USA). Maltohexaose was donated from Nihon Shokuhin Kako (Tokyo, Japan). Cellulase Y-C was purchased from Seishin Pharmaceutical (Tokyo, Japan). Xyloglucan octaose (XOS 9) was purified in our laboratory to a purity ≥ 98%. Tween 80, isopropyl myristate (IPM), gum arabic, soluble starch, and other required chemicals were purchased from Nacalai Tesque (Kyoto, Japan). The water used was generated with an ion-exchanger (> 18.2 MΩ, Direct-Q® 3UV, Millipores SAS, Molsheim, France).

2.2. Preparation of X-MSs and their isolation. A slurry of tamarind seed xyloglucan (2 g) with 1%, w/v was dissolved in 200 ml of sodium phosphate buffer (50 mM, pH 6.0), heated by microwave radiation, and vigorously stirred until boiling 2–3 times to ensure a homogeneous phase. Digestion with cellulase Y-C was further carried out at 37 °C using 9.5 enzyme units and incubated for 2 h. The sample was heated at 121 °C for 15 min to inactivate the enzyme. After cooling, the sample was centrifuged at 11,300 ×*g* for 30 min and then filtered through a 0.2-μm mixed cellulose ester membrane to remove insoluble pellets. Thereafter, the sample was dialyzed with a Spectra/Por®6 membrane with a molecular weight cutoff of 2 kD against water to discard glucose and oligosaccharide, with an average degree of polymerization (DP) less than 12, and subsequently desalted by a manually packed ion-exchange column (amberlite MB4, Organo, Tokyo, Japan). Next, 60% by volume of precooled methanol was added with continuous mixing for 1 h and left on ice water for an additional 2 h. The sediment was isolated

by centrifugation (13,000 ×*g*, 30 min) and dried to collect the sediment at a ≤ 60% fraction (later defined as X-MS DP 56). The supernatant was evaporated to decrease the volume, and precooled methanol at 70% of the final volume was then added and mixed to collect the sediment of the (60–70)% fraction. This step was repeated twice but with different methanol contents, namely, (70–80)% and (80–95)%. The last fraction was determined as X-MS DP 16. All fractions were dried using a lyophilizer (Eyela FDU-1200, Tokyo, Japan). The four obtained samples were profiled by Dionex HPAEC-PAD (4 × 250 mm CarboPac™ PA1 column, Dionex, Sunnyvale, CA, USA) (eluent: 16 mM sodium hydroxide for 20 min and further increased to 200 mM with a sodium acetate gradient solution of 0–100 mM for 40 min and from 100–250 mM for 20 min). Accordingly, the profiled peaks of only two samples (X-MS DP 16 and 56) did not overlap with each other and were therefore considered for use in the entire study. XOS 9 was purified from completed cellulase Y-C digests by preparative HPLC on an Imtakt Unison US-Amino column (20 × 250 mm). Eluent: 70%, v/v acetonitrile in water at a flow rate of 4 mL/min. Upon evaporation of the solvent, the XOS 9 powder was obtained by lyophilization. The chromatogram was reanalyzed by HPAEC-PAD.

2.3. Molecular weight and DP determination. The molecular weight of X-MSs was determined using a gel filtration HPLC (SB-803 HQ Shodex OHpak, 8.0 × 300 mm) eluted with sodium nitrate solution (0.1 M) at 0.5 mL/min, and the signals were detected by a refractive index detector (RI 2013 Plus, Tokyo, Japan). The molecular mass markers used were Shodex® standard P-82 pullulans (Showa Denko K.K., Kanagawa, Japan).

2.4. Monosaccharide composition. X-MSs (0.5 mg) were hydrolyzed at 120 °C in 0.1 mL of 2 M trifluoroacetic acid for 2 h in a glass vial. The acid was vaporized by nitrogen flushing. The sample was dissolved in water and analyzed by HPAEC-PAD under isocratic conditions of 16 mM sodium hydroxide to analyze the monosaccharide composition with myo-inositol internal standard. Normalized molar percentages relative to known sugar standards from each peak were obtained. DP was calculated by summation of the molar percentages of hexoses (glucose and galactose) and pentoses (arabinose and xylose), and the equation was expressed as (MW–18)/[(%hexose × 162/100) + (%pentose × 132/100)], whereas MW was the molecular weight obtained in Section 2.3. The molecular weight of a hexose residue in the X-MS chain is assumed to be 162 g/mol (180–18 for loss of water), and pentose is 132 g/mol obtained from 150–18.

2.5. Phase solubility assay of quercetin. X-MSs (100 μL) in series concentrations (0, 2, 4, 6, 8, and 10 mg/mL) were mixed well with excess quercetin (1 mg) at 25 °C for 6 h in triplicate. The samples were centrifuged three times at 12,000 ×*g* for 10 min. The supernatant portion was diluted in dimethyl sulfoxide, and the absorbance was measured at 381 nm by a UV–visible spectrophotometer (U2900, Hitachi, Tokyo, Japan). The concentration of quercetin in the supernatant was calculated using the calibration plot. The apparent equilibrium constant (K_S) was determined by following previous methods (Lang et al., 2014, 2022b).

2.6. Screening of the excipients. The maximum solubility of quercetin in several pure components of PEGs (200–550 Dalton), Tween 80, glycerol, IPM, and the combination with water of PEGs (1,000–8,000 Dalton) and X-MS DP 56 was evaluated according to the previous methods described in Section 2.5.

2.7. Hydrophobic interaction of TNS with X-MSs, TNS with X-MS DP 16 and Tween 80, TNS with Tween 80 and PEG 550. The complexes of 0.5 μM TNS with X-MS DP 16 (0, 0.5, 1, 3, 5, 8, 10, 12, 14, 16, 18, and 20 mg/mL) and X-MS DP 56 (0, 0.4, 0.6, 0.8, 1, 2, 3, 4, 5, 6, 7, 8, 9, and 10 mg/mL) in water were prepared by mixing them for 30 min in the dark at 25 °C and then transferred into 96-well black plates. The emission spectra were recorded by a fluorescence microplate reader (Tecan, Infinite M200-HAFH, Tokyo, Japan) at an excitation wavelength of 360 nm, and the fluorescence intensity was read at 430 nm for all experiments. The stability constant (K_c) was calculated according to the methods of Buranaboripan, Lang, Motomura, & Sakairi (2014) and Lang et al. (2022b). Tween 80 stock was prepared to 0.2 mg/mL and then diluted to the range of 0.001–0.1 mg/mL (including 0.001, 0.002, 0.003, 0.004, 0.005, 0.006, 0.007, 0.008, 0.009, 0.010, 0.015, 0.02, 0.03, 0.04, 0.05, 0.06, 0.07, 0.08, 0.09, and 0.1 mg/mL) in 96-well black plates. Fluorescence spectra for the complex formation with TNS were recorded with those Tween 80 ranges and those ranges with the addition of two concentrations of X-MS DP 16 (5 and 10 mg/mL) and PEG 550 (10 and 30 mg/mL). The determination of the critical micelle concentration (CMC) value was carried out by plotting the log Tween 80 concentrations against the fluorescence emission intensity. Two straight lines were drawn through these points, and their intersection was taken as the CMC.

2.8. Preparation of P0 and P14 microemulsions. Quercetin was dissolved in a series of concentrations in pure PEG 550 at 50, 100, 150, and 200 mg/mL. The last concentration was used routinely as the stock solution. Tween 80 was warmed at 60 °C in a heat box only when

needed to transfer to the tubes, whereas all samples were mixed at 25 °C. P0 was formulated by mixing PEG 550, Tween 80, IPM, an aqueous solution of 5% X-MS DP56 in water, and water in a volume fraction of 20:70:10:60:160 μL (having a final volume of 320 μL). For the comparison of saccharide excipients, the following maltohexaose, CDs, XOS 9, X-MS DP 16, soluble starch, gum arabic, and dextran T 40 were prepared in 5%, w/v solution and introduced to the P0 formula by replacing the portion of X-MS DP56 (60 μL). The samples were mixed vigorously and incubated at 25 °C in the dark overnight before the appearance was visualized. Centrifugation was performed to remove unloaded quercetin. The ternary phase diagram was constructed based on the P0 formulation without the addition of quercetin and X-MS. The PEG 550 volume increased from 20 μL to 20, 30, 40, and 50 μL; IPM from 10 μL to 10, 20, and 30 μL; and Tween 80 from 70 μL to 70, 80, and 90 μL. Subsequently, a one-equal volume of the sample by water was added to the medium, yielding 36 formulation trials. A visual assessment of transparency was performed to define the microemulsion zone in the ternary diagram. The type of microemulsion in P0 was identified when water-in-oil (W/O) medium was first prepared from IPM, PEG 550, and Tween 80 (1:2:7 mL to total 10 mL in a glass tube placed in a 25 °C water bath), and the fixed amount of pure water (1 mL each) was then titrated. Conductivity measurements were performed using a TOA EC meter CM-14p model (TOA Electronics, Japan).

P14 tests were composed of the same above components of 40:90:10:60:200 μL (having a final volume of 400 μL), whereas 5%, w/v aqueous solution of X-MS DP 16, 56, dextran T 3.5, and T 6 were placed in the 60-μL portion. The template microemulsion was prepared without the addition of quercetin but maintained in volume with PEG 550. The droplet sizes were characterized after aqueous dilution 50 times via dynamic light scattering in triplicate by a Zetasizer μV series from Malvern Instruments (Worcestershire, UK).

2.9. TEM analysis. Quercetin-loaded microemulsion (P0 formula) with X-MS DP 56 was diluted with water 100 times to determine the particle size and shape by a JEM-2100 transmission electron microscopy (TEM, JEOL, Tokyo, Japan). One drop of the formulation was placed on a formvar-coated copper grid. A drop of a 2% aqueous solution of uranyl acetate was subsequently placed onto the grid for negative staining to improve the contrast and allowed 30–60 s until drying. An image was obtained using 300,000× magnification.

2.10. Antioxidant assays. Four quercetin-loaded sample solutions, including two megalomeric microemulsion, X-MS DP 16 and 56, the template microemulsion without X-MS, and methanol,

were prepared with appropriate quercetin ranges (0, 10, 20, 40, 60, 80, and 100 μg/mL). Sodium phosphate buffer (pH 6.0 and 7.4; 40 mM, 80 μL) and the samples (20 μL) were added to the 96-well plate, and the stock solution of DPPH prepared in methanol (0.2 mM, 100 μL) was transferred to the plate by a multichannel pipette and mixed by tips one time. The samples were incubated at 25 °C in the dark for 30 min. The absorbance was recorded at 517 nm by the Tecan microplate reader. The ABTS assay was performed according to the method guideline of Xiao, Xu, Lu, & Liu (2020) with some modification. Briefly, stock solutions of ABTS (7 mM) and potassium persulfate (2.45 mM) were prepared separately in acetic acid buffer (50 mM, pH 4.0). The ABTS reaction solution was prepared by mixing each stock volume of 5 mL and maintained at 25 °C for 16 h in the dark to oxidize ABTS to $ABTS^{\bullet+}$ radicals. The ABTS solution of 2.8 mL was diluted to 65 mL of 50% methanol in 50 mM sodium acetate buffer (50 mM, pH 4.0) to obtain the ABTS working solution and maintained at 25 °C for 30 min in the dark. The ABTS assay was performed by adding ABTS working solution (190 μL) to samples (10 μL) in 96-well plates and incubating at 25 °C in the dark for 30 min. The absorbance was recorded at 734 nm. The measurements were performed in triplicate. Radical scavenging (%) was calculated according to the equation: $A_3 – (A_1 – A_2)/A_3 \times 100$, where the absorbance of free radicals plus the sample solution was recorded as A_1, the absorbance of methanol plus the sample solution was recorded as A_2 (blank), and the absorbance of free radicals plus methanol solution was recorded as A_3. The regression equation was estimated from plots of %Scavenging (Y-axis) against quercetin concentration (X-axis), and IC50 was calculated from (50–Y-intercept)/slope.

2.11. Statistical analysis. Differences among treatment groups were analyzed with the Tukey–Kramer and Student's *t* tests after one-way ANOVA. A P value of less than 0.05 was considered significant.

3. Results and Discussion

3.1. Isolation of active X-MSs by enzymatic hydrolysis. Based on the structural configuration, Janado & Yano (1985) suggested that two aldopentoses, D-xylose and L-arabinose, predominantly possess superior hydrophobicity among other monosaccharides, such as D-galactose and D-glucose, whereas the cellulose skeleton can laterally stack via hydrophobic interactions and form a sheet-like structure (Miyamoto et al., 2009). Accordingly, tamarind seed xyloglucan underlying these patterns was predicted to have the potential to enhance the water solubility of water-insoluble substances. However, polymeric xyloglucan forms molecular

aggregates even in very dilute solutions, and the solution after heating is highly viscous. In this study, we established a method to partially cleave and purify xyloglucan into two nonoverlapping MS sizes to evaluate the role of chain length degree in the stabilized SMES. *Trichoderma viride* cellulase (EC 3.2.1.4) acting as endo-β-(1→4)-glucanohydrolase hydrolyzed xyloglucan at a 2-h incubation to a mixture of four repeating units of xyloglucan oligosaccharides (XOSs: XXXG, XLXG, XXLG, and XLLG with a retention time of 49–55 min) and a large number of MS (68–83 min), as depicted in the HPAEC-PAD chromatogram (Fig. 1A, top). We proposed an enzyme mechanism involving the cleavage of random internal β-(1→4)-glucan at the unsubstituted parts and further access to more highly substituted regions. Therefore, the incubation time was a critical criterion to determine the chain length of X-MS. For instance, the incubation time at 40 min, 1 h, and 2 h enabled X-MS DPs of 122, 73, and 28, respectively. After further prolonged incubation, XOSs eventually became prominent. Isolation of those resulting mixtures of X-MS fragments to DP 16 and 56 by a series of consecutive steps of methanol concentrations was successful as envisaged with nonoverlap peaks by HPAEC-PAD (Fig. 1A, bottom). The composition analysis later revealed four types of sugar elements, arabinose, galactose, glucose, and xylose, from native xyloglucan (255,113 Dalton) with molarity percentages (mol%) of 4.7, 22.6, 44.3, and 28.5, respectively. X-MS DP 16 has the shortest size, with a molecular weight of 2,488 Dalton and mol% values of 1.7, 21.1, 44.5, and 32.7. X-MS DP 56 is longer, with 8,493 Dalton and mol% values of 3.4, 23.0, 42.9, and 30.6, respectively. Gel filtration HPLC analysis indicated that X-MS DP 16 and 56 have a better peak profile than parental xyloglucan (Fig. 1B). The sugar compositions of X-MS were similar to those of the native xyloglucan but only lower for arabinose content. The arabinose content in X-MS DP 16 may be negotiable as well as lacking in those repeating units of XOSs. The arabinose substituent plays a structural role in a highly viscous solution. Consequently, both X-MSs exhibited improved solubility in water. Preparation of the X-MS DP 16 solution did not require a rise in temperature for complete dissolution. The DP 56 solution required slight heating; however, it did not form an aggregate in water afterward. The fine components in X-MS molecules were identified by long incubation with the fungal cellulase. The results in HPAEC-PAD indicated that X-MS DP 16 and 56 were enriched in small building blocks of the XXXG, XLXG, XXLG, and XLLG collection with some slight free glucose (data not shown). However, some other unknown shorter XOS fragments and larger resistance molecules were also detected. The model structures of X-MSs are proposed in Fig. 1C. X-MS DP 16 may contain two repeating XOSs, whereas DP 56 has six repeating XOSs with more galactose and arabinose contents. This emphasized the existence of amphiphilicity. The hydrophobic property of X-MS

307 is derived from a large number of xylosyl side chains and additional arabinose molecules
308 substituted in the cellulose backbone, whereas galactose residues facilitate aqueous solubility.
309 Vincken, Keizer, Beldman, & Voragen (1995) demonstrated that the minimum length of at least
310 four repeating units of xyloglucan fragment was required to enable in vitro adsorption of
311 xyloglucan molecules to cellulose microfibrils, whereas XOS with one or two repeating units
312 did not adsorb. Kabel, van den Borne, Vincken, Voragen, & Schols (2007) removed arabinosyl
313 and *O*-acetyl substituents on xylan and found that the adsorption of xylan to cellulose was
314 increased. Hence, in addition to size, the side chain configuration also contributes to the
315 hydrophobic property of X-MS.
316
317 **3.2. Interaction of X-MS and PEG 550 in Tween 80 micelles.** X-MS is an amphiphilic
318 saccharide that possesses both hydrophilic and hydrophobic regions, but the functional groups
319 of the hydrophilic head groups and hydrophobic tail groups were not as well defined as those of
320 Tween 80 molecules. The interaction between Tween 80 with X-MS DP 16 and Tween 80 with
321 PEG 550 was analyzed by fluorescence spectroscopy with a TNS probe. TNS is practically
322 nonfluorescent in an aqueous solution but undergoes a large fluorescence enhancement in
323 appropriate hydrophobic environments or some regions of low polarity (Beyer, Craig, &
324 Gibbons, 1973). Binding interactions of X-MSs with TNS were first determined. The
325 fluorescence emission spectra of TNS at increasing concentrations of X-MS DP 16 and 56 were
326 recorded, and both emission maxima were accordingly detected at 430 nm (Fig. 2A and 2B).
327 The K_c was determined by the double-reciprocal plots (Fig. 2A and 2B; inset) according to the
328 Benesi-Hilderbrand equation ($R^2 > 0.99$), which yielded K_c values of 127 and 180 M^{-1} for X-MS
329 DP 16 and DP 56, respectively. Tween 80 does not have a specific fluorescence spectrum, and
330 the intensity of emission fluorescence is weak. However, the long alkyl chain of Tween 80 in
331 water can self-assemble and form a hydrophobic microenvironment at a CMC of 0.015 mg/mL
332 (log CMC = -1.824). Two concentrations of X-MS DP 16 at 5 and 10 mg/mL were added to
333 TNS solutions with a series concentration of Tween 80 from 0.001–0.1 mg/mL. It was found
334 that the addition of X-MS DP 16 did not alter the CMC value (Fig. 2C), but the TNS intensity
335 was enhanced slightly at low concentrations of Tween 80. At the Tween 80 monolayer (<
336 CMC), X-MS exhibits a strong interaction with TNS based on the increasing X-MS
337 concentrations. Above the CMC, the intensity of TNS increased greatly with increasing
338 concentrations of Tween 80. X-MS binds with Tween 80 molecules at the inner micelles as the
339 intensity increases rapidly. However, increasing the X-MS concentrations had a small effect on
340 the hydrophobic polarity, as the intensity does not increase in proportion to the X-MS

concentrations. Notably, the size of the Tween 80 micelles was assumed to not continue to increase, which may restrict the encapsulation of the extra X-MS density. Our results demonstrated that the X-MS branch molecules incorporate to form a hydrophilic outer shell and hydrophobic inner core of Tween 80 micelles, the so-called cosurfactant, and further increase the core stability.

PEG 550 was the most prominent solubilizer for quercetin dissolution before SMES was formulated. Thus, we identified the stimulatory role of PEG 550 in the PEG-associated micelles. PEG is hydrophilic and distributes at the surface layer of the micelle corona structure (Agrawal, Tatode, Rarokar, & Umekar, 2020). It may locally induce polarity in Tween 80, which makes the environment slightly polar inside the micelles, and consequently, the hydrophobic environment becomes less hydrophobic. As shown in Fig. 2D, the TNS intensity in the solutions containing PEG 550 and Tween 80 remained constant and was the same as that of the solution containing only Tween 80 when the Tween 80 molecule had not yet formed micelles (< CMC). The quenching of TNS fluorescence was observed when PEG 550 participated in the micellization process (> CMC), as the intensity is always less than that of the solution containing only Tween 80. The results implied that PEG 550 does not impact the micellular stability, as the low molecular weight PEG were not hydrophobic enough to bind with a surfactant molecule (Dhara & Shah, 2001). The role of PEG molecular weight on the solubility enhancement of quercetin was subsequently considered in the next section.

3.3. Screening of excipients for SMES formulations. Quercetin is practically insoluble in water (6 μg/mL). Hydrophobic interactions between quercetin and X-MS were responsible for the solubility improvement of quercetin, increasing its apparent water solubility by 4.8- and 5.8-fold with 10% (w/v) X-MS DP 16 and 56 solutions, respectively. The K_S calculated from the phase solubility diagram was found to be consistent with X-MS chain length, as the K_S increased from 114 to 677 M^{-1} for X-MS DP 16 and 56, respectively. To date, dimethyl sulfoxide and alcohol are the most common organic solvents for quercetin dissolution. They are practically used in in vitro cellular tests with the maximum solubility for quercetin at 30 and 2 mg/mL, respectively ("Product Information," 2020). However, quercetin immediately precipitated after aqueous dilution, and dimethyl sulfoxide is not permissible in pharmaceutical formulations. In this study, preformulation studies were carried out to guide the appropriate selection of SMES ingredients. PEG is a synthetic polyether with a commercially broad molecular weight ranging from 200 to 4,000,000 Dalton (Biondi, Motta, & Mosesso, 2002; Dhara & Shah, 2001; Sun, Zhang, & Chu, 2008). PEGs are widely used as a vehicle or base in

foods, cosmetics, and pharmaceuticals as they are FDA-approved (Sermkaew & Plyduang, 2020). The lower the PEG molecular weight is, the higher the hydrophilic properties, as the ratio of terminal hydroxyl end and polyethylene groups increases. In our study, an excess amount of quercetin powder was mixed vigorously with short-chain PEGs of varying molecular weights (200, 300, 400, 550 Dalton), glycerol, Tween 80, and IPM oil. The aqueous phase was subsequently collected to evaluate their maximum quercetin solubility. It was found that those values of quercetin are the best among the short molecular weight series of PEG (200–550 Dalton) between 196.62 ± 0.55 and 204.57 ± 1.37 mg/mL and much higher compared with glycerol (2.60 ± 0.12 mg/mL) and Tween 80 (6.30 ± 0.14 mg/mL) (Table 1), as well as the value found in the literature (14.12 ± 2.18 μg/mL for PEG 400) (Sermkaew & Plyduang, 2020). Although PEG 400 is the most commonly used coemulsifier in drug formulation (Baksi et al., 2018; Gao et al., 2009; Sermkaew & Plyduang, 2020), PEG 550 was selected for use entirely because it was the best quercetin solubilizer compared with other solvents, including the combination with water, Tween 80, and X-MS DP 56. Polymeric PEGs with longer sized chains, 1000, 4000, 6000, and 8000 Dalton, and X-MS were only tested after being dissolved in water, as they are solid in form. Notably, the combination with water decreased the degree of quercetin solubilization. For instance, 20% PEG 550 in water could dissolve quercetin at only 0.16 ± 0.01 mg/mL, a 1,275-fold decrease compared with pure PEG 550 (203.80 ± 1.37 mg/mL). Tween 80 is a preferred nonionic emulsifier that has low toxicity. The addition of 10% (w/v) X-MS in water and 10% (v/v) Tween 80 in water was found to increase the quercetin solubility from 0.16 ± 0.01 to 1.38 ± 0.25 mg/mL and 2.51 ± 0.03 mg/mL, respectively. This result emphasized the combined role of Tween 80 and X-MS in the water phase, which could have a synergistic effect with PEG 550 for quercetin solubility. Emulsifiers generally stabilize W/O microemulsions with hydrophilic-lipophilic balance (HLB) values between 4 and 6, whereas for O/W microemulsions, the value is between 8 and 18 (Pichot, Spyropoulos, & Norton, 2010; Syed & Peh, 2014). For effective emulsification in an SMES, specific oils require emulsifiers having a specific HLB (polar or nonpolar characteristic). The HLB values of emulsifiers are mostly preferred to be approximately similar to those of the respective oils to achieve maximum stabilization. The HLB value of Tween 80 is 15; therefore, a high required HLB (RHLB) oil phase, such as IPM (with RHLB 11.5), may be more feasible to formulate O/W SMES. IPM is a low-viscosity oil synthesized from isopropyl alcohol and myristic acid, a naturally occurring fatty acid. We evaluated the maximum solubility of quercetin in pure IPM with the same procedure, which was 0.28 ± 0.01 mg/mL. Accordingly, formulations with Tween 80, PEG 550, X-MS, and IPM were evaluated for quercetin-loaded SMES.

3.4. Evaluation of the P0 formula for quercetin loading and its microstructure. In our preliminary trial, one formulation was well established with PEG 550, Tween 80, IPM, an aqueous solution of 5% X-MS DP 56 in water, and water in the volume fraction of 20:70:10:60:160 μL (having a final volume of 320 μL), namely, P0. The final mass percentages of PEG 550, Tween 80, IPM, and water in P0 were 6.25, 21.9, 3.12, and 68.8, respectively, with the addition of 0.94% X-MS DP 56 component. Medium before and after the addition of 160 μL of water was categorized as bicontinuous microemulsion (37.5% water; total volume 160 μL) and O/W (68.8% water; total volume 320 μL) medium, respectively, as discussed later. The loading capacity of quercetin in P0 was compared using two methods: (i) from dissolved quercetin form and (ii) from quercetin powder. According to (i), quercetin was initially dissolved in PEG 550 in series concentrations of 50, 100, 150, and 200 mg/mL. A fixed portion (20 μL) of those four series would mix with the medium in a total volume of 320 μL, yielding ideal quercetin loads of 3.13, 6.25, 9.38, and 12.5 mg/mL, respectively. The experiments were performed with a fixed 20-μL quercetin concentration series mixed well with bicontinuous medium containing Tween 80, IPM, and water (70, 10, and 60 μL, respectively), and one equal volume of water (160 μL) was then added as a continuous phase. It was found that the four series suspensions are all clear both in the bicontinuous phase and after the addition of water (160 μL). After standing overnight, the suspension with portions of 50 and 100 mg/mL quercetin in PEG 550 was still clear yellow, but the latter 150- and 200-mg/mL samples became turbid. This result indicates that in the last two samples, quercetin was overloaded and led to precipitation. After centrifugation, the quercetin concentration in the supernatant was 6.8 ± 0.5 mg/mL, meaning that P0 could be sufficient to have that load as a maximum. Next, X-MS DP 56 (5%, w/v solution) was applied to P0, replacing the water portion (60 μL), and followed the identical protocol. Four portions of the 50–200-mg/mL quercetin series, Tween 80, and IPM were all turbid after mixing with X-MS DP 56 in bicontinuous medium. However, after the bulk water (160 μL) was added, all samples became clear yellow in color and remained stable for over a month. This result indicated that the addition of X-MS DP 56 could stabilize a full load of quercetin at 12.5 mg/mL without precipitation. (ii) In contrast, the direct addition of quercetin powder into the fixed quantity of P0 medium maintained quercetin at only 2.0 ± 0.2 mg/mL, emphasizing the solubilizing role of quercetin with PEG 550 as the main strategy to overcome the poor solubility of quercetin. We strongly recommend not to alternate the methods of (ii) and (i).

Among lipid formulations, SMES requires a highly specific balance formulation. The ternary phase diagram was initially constructed based on the P0 formulation. PEG 550 volume was the most critical factor, as it determines the concentration of quercetin loading in each formulation. Among the 36 formulations located in the pentagon area in Fig. 3A, only the green area (18 samples) was found to be a microemulsion. This means that the composition with low IPM, low PEG 550, and a sufficiently large amount of Tween 80 was the desired ratio to obtain the microemulsion template. Next, we replaced the compositions in the green area with the portions of 200 mg/mL quercetin in PEG 550 and 5% X-MS DP 56 solution instead of pure PEG 550 and water to test the full quercetin load, which is proposed to range from 15.79 to 23.53 mg/mL. However, such samples were precipitated after standing overnight. This indicates that a high concentration of quercetin could influence the emulsification region. Among those tested formulations, P14 marked inside of the green area with the full load of 20 mg/mL quercetin was used to test the improved loading in Section 3.5.

Conductivity measurements were carried out to determine the makeup of the water phase of the P0-based formulation: W/O emulsions are nonconductive, whereas O/W emulsions are conductive. At the first state, the incomplete P0 was W/O medium, as the initial conductivity was very low (0.031 mS/m). Then, after titration with water to 37.5%, the conductivity was 13.67 mS/m, which was consequently classified as a bicontinuous medium. The conductivity values were plotted against the water content in micelles, as shown in Fig. 3B, demonstrating three different structural types of W/O, bicontinuous structures (B.C.) and O/W. The conductivity of the sample rapidly increased to a maximum of 41.1 mS/m after 71.4–72.2% water was introduced and then started to decrease. The result indicates that the P0 medium with 68.8% was an O/W microemulsion (carrying a conductivity of 40.5 mS/m) as water became a continuous phase and the conductivity almost reached the maximum value zone. The latter decrease was O/W with excess water.

3.5. Loading capacity of quercetin in P0 and P14 containing various saccharides. Most saccharides are considered to be hydrophilic molecules since a large number of hydroxyl groups are present. Alternatively, the hydrophobic properties derived from the nonpolar methine patches in monosaccharides are possibly stronger if the stereochemical constraints on the chain transform into a better conformation. In this study, we carefully isolated X-MS as an amphiphilic substance with a strong hydrophobic characteristic. The influence of different types of saccharides on the loading capacity of quercetin in P0 was evaluated as a comparison. The solution stocks of 5% (w/v) of four oligosaccharides, including maltohexaose, CDs (α-, β-, and

γ-CDs), XOS 9, X-MSs (DP 16 and 56) and three polysaccharides, including soluble starch, gum arabic, and dextran T 40, were introduced to P0 by replacing the portion of 60 μL of water (used as a control). The SMES medium was evaluated by visual assessment and centrifuged to detect quercetin in the supernatant, and the results are shown in Table 2. The PEG 550 portion determined the load of quercetin, as quercetin was initially dissolved in PEG 550 at a fixed concentration (200 mg/mL). If no precipitation was found, a full load of quercetin in SMES was suggested to be 12.5 mg/mL. Here, we first evaluated the soluble capacity of that PEG 550 portion only in a continuous phase. The portion of quercetin in PEG 550 was poured into water instead of P0 medium. The precipitation of quercetin immediately occurred. Only 0.11 ± 0.15 mg/mL quercetin in the supernatant could be detected. Next, the portion was poured into P0 using water (control) instead of saccharides, following the steps of Tween 80, IPM, and water. In this case, 6.8 ± 0.50 mg/ml quercetin was detected, meaning that in the colloidal solution, quercetin could be more appreciably encapsulated. Between oligosaccharides and polysaccharides, XOS 9 and soluble starch were the most effective saccharides, in which a small quercetin precipitate was found, whereas quercetin in the other samples was highly cloudy and precipitated. The megalomeric microemulsion with X-MSs displayed a better load among all samples. SMES containing X-MS DP 56 had a clear appearance with a full load of quercetin, whereas X-MS DP 16 had very slight precipitates.

To increase the load of quercetin in tests, the portion of quercetin in PEG 550 (fixed at 200 mg/mL) must be increased correspondingly. Accordingly, the composition in P14 was composed of PEG 550, Tween 80, IPM, an aqueous solution of two types of MS in water (dextran T and X-MS with 1, 5, 10, 15, and 20%), and water at the ratio of 40:90:10:60:200 μL (having a final volume of 400 μL). The final mass percentages of PEG 550, Tween 80, IPM, and water in P14 were 10.0, 22.5, 2.50, and 65.0, respectively, with additional MSs ranging from 0.15–3.0%. The full load of quercetin was 20.0 mg/mL. Fig. 4A presents an image of the samples in which the dissolved quercetin was added into a P14 template containing two sizes of X-MS and dextran T MS. Dextran T MS is a commercially available hydrophilic linear-isomaltomegalosaccharide with a main α-(1→6)-linked D-glucopyranose chain. Here, we used dextran T MS with two molecular weights 3,500 Dalton for T 3.5 and 6,000 Dalton for T6. X-MS DP 16 and 56 with molecular weights of 2,488 and 8,493 Daltons, respectively, were again used. In the control set (without the addition of MSs), P14 had a drug load of 7.1 ± 0.6 mg/mL, with no significant ($p > 0.05$) relationships with those of dextran T 3.5 and T 6 (Fig. 4B). Fully coarse precipitates were observed at all sample concentrations. In contrast, it was likely that a growing mass of X-MS DP 16 until 2.25% was required to achieve a high load of quercetin at

17.09 ± 0.83 mg/mL, and further loading was then not possibly improved even by the mass increase. In contrast, the high load of quercetin immediately reached 17.70 ± 0.40 mg/mL even with only a tiny amount of X-MS DP 56 (0.15%). Slightly increasing X-MS DP 56 to 0.75% eventually yielded the maximum quercetin solubility at 18.30 ± 1.42 mg/mL. Further increase was not necessary for the load; however, in turn, X-MS DP 56 tended to aggregate instead as fine precipitates were observed. This may be explained by the shorter chain length of X-MS DP 16 that could participate in the micelles with the higher masses and concentrations required for quercetin loading. However, the large molecule of X-MS DP 56 was relatively full and required only in low amounts, and only a small concentration was sufficient for the load. The influence of X-MS chain length and concentration on the particle sizes of the megalomeric microemulsion is presented in Fig. 5A. The largest microemulsion template consisted of quercetin and X-MS (12.6 ± 0.3 nm), with a moderate size distribution (polydispersity index (PDI) = 0.20 ± 0.03). With a larger X-MS size (at 3.0% final concentration), the diameters were 12.7 ± 0.2 and 12.1 ± 0.0 nm for X-MS DP 16 and 56, respectively. With quercetin loading, both megalomeric microemulsion sizes were further reduced. However, increasing the concentrations of X-MS DP 56 was not likely to change the sizes, as it was in the average droplet sizes of 11.5 nm (with PDI of 0.04–0.09). With X-MS DP 16 and quercetin loading, the size slightly increased from 11.5–11.8 nm (with PDI of 0.03–0.10). The micelle was likely not able to expand, in agreement with the results discussed earlier. The TEM micrograph (Fig. 5B) confirmed the globular diameter without aggregation. However, the cylindrical shape of the micelles also appeared consistent with a previous study (Aizawa, 2009). The attempts of improving loads of quercetin in lipid-based carriers have been seriously investigated, as well as of decreasing the particle size to allow better absorption. Hädrich et al. (2016) developed the best SMES with 20-nm droplets using a hot solvent diffusion technique with less emulsifier (1.5% PEG 660-stearate) but still incorporated only 1.5 mg/mL quercetin. Gao et al. (2009) were able to incorporate a higher quercetin content of 4.138 mg/mL in a droplet size of 38.9 nm, but the formulation consisted of a relatively high Tween 80 concentration (48%, w/w). Our megalomeric microemulsions have more advantages, as they incorporate a larger amount of quercetin (12.5–18.3 mg/mL) with smaller droplets, whereas lesser emulsifier/coemulsifier amounts are used. P0 formulated with 6.25% PEG 550, 21.9% Tween 80, 3.12% IPM, 68.8% water, 0.94% X-MS DP 56 and a particle size of 11.6 ± 0.2 nm can sustain the load of 12.5 mg/mL quercetin without precipitation over a month. P14 with 10.0% PEG 550, 22.5% Tween 80, 2.50% IPM, 65.0% water, and 0.15% X-MS DP 56 and a particle size of 11.4 ± 0.1 nm was sufficient to hold the

higher load of 17.70 ± 0.40 mg/mL with a small precipitate in three days. Formulations and their loading capacity of megalomeric microemulsions are summarized in Scheme 1.

3.6. Antioxidation effect. The DPPH and ABTS assays are commonly applied to estimate the antioxidant activities of plant extracts. It was also very efficacious to identify the state of oxidation under different pH conditions and mimic a physiological fluid. ABTS is found to be stable from pH 3.0 to 6.5. Then, we performed only the tests of ABTS at pH 4.0 and DPPH at 6.0 and 7.4 (Table 3), where the original pH values of the quercetin-loaded microemulsion with X-MSs were 5.8. Quercetin H-donor ability was not notably different among the quercetins in methanol and all megalomeric microemulsions based on ABTS assays. However, the antioxidant activity was found to be much improved by the microemulsion containing X-MS DP 16 and 56 for DPPH assays, with values of 22.2 ± 1.6 and 24.1 ± 1.2 μg/mL, respectively. Although the formulation containing X-MSs could be able to ensure that the antioxidant activity against DPPH and ABTS was maintained compared to the behavior in methanolic solution, the presence of X-MS in the microemulsion has more potent antioxidant properties for DPPH at both pH values but not for ABTS. Since the interactions among different antioxidant components can be synergistic especially between quercetin and X-MS in the oil phase nearly the surfactant film, the antioxidant mechanism and activity in the presence of X-MSs toward the variation of free radicals will be great insight in the following work.

4. Conclusion.

The lack of fundamental knowledge derived from unavailable MS-size preparation on the influence of SMES properties seriously hinders development in the field of food supplements, pharmaceutical applications, and even carbohydrate research. X-MS is a branch saccharide amphiphile. The hydrophobic region occurs naturally from methine (CH) groups of the sugar monomers, especially xylose and arabinose residues. X-MS probably has a weaker hydrophobic characteristic, and X-MS itself displayed a slight effect on quercetin binding. However, the implementation of X-MSs toward SMES was highly compatible, as X-MS molecules were confined in micellular solutions depending on the sizes. Additionally, we found that PEG 550 displays excellent efficiency in dissolving quercetin, especially in determining the load of quercetin in the formulations. We carefully chose X-MS to prepare megalomeric microemulsions with two formulations. P0 could sustain the load of 12.5 mg/mL quercetin without precipitation over a month. P14 was sufficient to hold the higher load of 17.70 ± 0.40

mg/mL with a small precipitate for three days. This is the first study that explained how effective X-MSs were able to stabilize quercetin in the microemulsion.

CRediT authorship contribution statement

Weeranuch Lang: Conceptualization, Investigation, Formal analysis, Writing - original draft, review & editing. Debashish Mondol: Writing - original draft, Investigation, Methodology. Aphichat Trakooncharoenvit: Methodology, Formal analysis. Takayoshi Tagami: Resources, Supervision. Masayuki Okuyama: Data curation, Resources. Tohru Hira: Supervision, Resources. Nobuo Sakairi: Conceptualization, Supervision, Writing - review & editing. Atsuo Kimura: Supervision, Funding acquisition, Project administration.

Declaration of competing interest. The authors have no conflicts of interest to declare.

Acknowledgments

We thank the staff of the Instrumental Analysis Division of the Creative Research Institution at Hokkaido University for performing mass spectrometry analysis and Mr. Toshiaki Itou at the facility area of Emission Electron Microscope, Research Faculty of Agriculture, Hokkaido University, for performing the TEM analysis. We thank Elsevier's language editing services for final English proofreads.

References

Agrawal, R. D., Tatode, A. A., Rarokar, N. R., & Umekar, M. J. (2020). Polymeric micelle as a nanocarrier for delivery of therapeutic agents: A comprehensive review. *Journal of Drug Delivery and Therapeutics*, *10*, 191–195. https://doi.org/10.22270/jddt.v10i1-s.3850.

Aizawa, H. (2009). Morphology of polysorbate 80 (Tween 80) micelles in aqueous 1,4-dioxane solutions. *Journal of Applied Crystallography*, *42*, 592–596. https://doi.org/10.1107/S002188980902295X.

Andrés, S., Tejido, M. L., Bodas, R., Morán, L., Prieto, N., Blanco, C., & Giráldez, F. J. (2013). Quercetin dietary supplementation of fattening lambs at 0.2% rate reduces discolouration and microbial growth in meat during refrigerated storage. *Meat Science*, *93*, 207–212. https://doi.org/10.1016/j.meatsci.2012.08.023.

Bai, L., & McClements, D. J. (2016). Formation and stabilization of nanoemulsions using biosurfactants: Rhamnolipids. *Journal of Colloid and Interface Science*, *479*, 71–79. https://doi.org/10.1016/j.jcis.2016.06.047.

610 Baksi, R., Singh, D. P., Borse, S. P., Rana, R., Sharma, V., & Nivsarkar, M. (2018). In vitro and
611 in vivo anticancer efficacy potential of Quercetin loaded polymeric nanoparticles.
612 *Biomedicine and Pharmacotherapy*, *106*, 1513–1526.
613 https://doi.org/10.1016/j.biopha.2018.07.106.
614 Beyer, C. F., Craig, L. C., & Gibbons, W. A. (1973). Structural requirements for binding and
615 fluorescence enhanement of th fluorescent probe TNS with peptides. *Nature New Biology*,
616 *241*, 78–80. https://doi.org/doi: 10.1038/newbio241078a0.
617 Biondi, O., Motta, S., & Mosesso, P. (2002). Low molecular weight polyethylene glycol
618 induces chromosome aberrations in Chinese hamster cells cultured in vitro. *Mutagenesis*,
619 *17*, 261–264. https://doi.org/10.1093/mutage/17.3.261.
620 Buranaboripan, W., Lang, W., Motomura, E., & Sakairi, N. (2014). Preparation and
621 characterization of polymeric host molecules, β-cyclodextrin linked chitosan derivatives
622 having different linkers. *International Journal of Biological Macromolecules*, *69*, 27–34.
623 https://doi.org/10.1016/j.ijbiomac.2014.05.016.
624 Crispín-Isidro, G., Hernández-Rodríguez, L., Ramírez-Santiago, C., Sandoval-Castilla, O.,
625 Lobato-Calleros, C., & Vernon-Carter, E. J. (2019). Influence of purification on
626 physicochemical and emulsifying properties of tamarind (*Tamarindus indica* L.) seed
627 gum. *Food Hydrocolloids*, *93*, 402–412. https://doi.org/10.1016/j.foodhyd.2019.02.046.
628 Dajas, F. (2012). Life or death: Neuroprotective and anticancer effects of quercetin. *Journal of*
629 *Ethnopharmacology*, *143*, 383–396. https://doi.org/10.1016/j.jep.2012.07.005.
630 Dhara, D., & Shah, D. O. (2001). Effect of poly(ethylene glycol)s on micellar stability of
631 sodium dodecyl sulfate. *Langmuir*, *17*, 7233–7236. https://doi.org/10.1021/la001030i.
632 Gao, Y., Wang, Y., Ma, Y., Yu, A., Cai, F., Shao, W., & Zhai, G. (2009). Formulation
633 optimization and in situ absorption in rat intestinal tract of quercetin-loaded
634 microemulsion. *Colloids and Surfaces B: Biointerfaces*, *71*, 306–314.
635 https://doi.org/10.1016/j.colsurfb.2009.03.005.
636 Hädrich, G., Monteiro, S. O., Rodrigues, M. R., de Lima, V. R., Putaux, J. L., Bidone, J.,
637 Teixeira, H. F., Muccillo-Baisch, A. L., & Dora, C. L. (2016). Lipid-based nanocarrier for
638 quercetin delivery: system characterization and molecular interactions studies. *Drug*
639 *Development and Industrial Pharmacy*, *42*, 1165–1173.
640 https://doi.org/10.3109/03639045.2015.1118491.
641 Hara, H., Kume, S., Iizuka, T., Fujimoto, Y., & Kimura, A. (2017). Enzymatically synthesized
642 megalo-type isomaltosaccharides enhance the barrier function of the tight junction in the
643 intestinal epithelium. *Bioscience, Biotechnology and Biochemistry*, *82*, 629–635.

https://doi.org/10.1080/09168451.2017.1398065.
Janado, M., & Yano, Y. (1985). Hydrophobic nature of saccharides as evidenced by their differential affinity for polystyrene gel in aqueous media. *Journal of Solution Chemistry*, *14*, 891–902. https://doi.org/10.1007/BF00646298.
Johari, J., Kianmehr, A., Mustafa, M. R., Abubakar, S., & Zandi, K. (2012). Antiviral activity of baicalein and quercetin against the Japanese encephalitis virus. *International Journal of Molecular Sciences*, *13*, 16020–16045. https://doi.org/10.3390/ijms131216785.
Kabel, M. A., van den Borne, H., Vincken, J. P., Voragen, A. G. J., & Schols, H. A. (2007). Structural differences of xylans affect their interaction with cellulose. *Carbohydrate Polymers*, *69*, 94–105. https://doi.org/10.1016/j.carbpol.2006.09.006.
Lang, W., Kumagai, Y., Sadahiro, J., Maneesan, J., Okuyama, M., Mori, H., Sakairi, N., & Kimura, A. (2014). Different molecular complexity of linear-isomaltomegalosaccharides and β-cyclodextrin on enhancing solubility of azo dye ethyl red: Towards dye biodegradation. *Bioresource Technology*, *169*, 518–524. https://doi.org/10.1016/j.biortech.2014.07.025.
Lang, W., Kumagai, Y., Sadahiro, J., Saburi, W., Sarnthima, R., Tagami, T., Okuyama, M., Mori, H., Sakairi, N., Kim, D., & Kimura, A. (2022a). A practical approach to producing isomaltomegalosaccharide using dextran dextrinase from *Gluconobater oxydans* ATCC 11894. *Applied Microbiology and Biotechnology*, *106*, 689–698. https://doi.org/10.1007/s00253-021-11753-6.
Lang, W., Kumagai, Y., Habu, S., Sadahiro, J., Tagami, T., Okuyama, M., Kitamura, S., Sakairi, N., & Kimura, A. (2022b). Physicochemical functionality of chimeric isomaltomegalosaccharides with α-(1 → 4)-glucosidic segments of various lengths. *Carbohydrate Polymers*, *291*, 119562. https://doi.org/10.1016/j.carbpol.2022.119562.
Liu, C. H., Huang, Y. C., Jhang, J. W., Liu, Y. H., & Wu, W. C. (2015). Quercetin delivery to porcine cornea and sclera by solid lipid nanoparticles and nanoemulsion. *RSC Advances*, *5*, 100923–100933. https://doi.org/10.1039/c5ra17423f.
Majee, S. B., Avlani, D., & Biswas, G. R. (2016). Non-starch plant polysaccharides: Physicochemical modifications and pharmaceutical applications. *Journal of Applied Pharmaceutical Science*, *6*, 231–241. https://doi.org/10.7324/JAPS.2016.601033.
Miyamoto, H., Umemura, M., Aoyagi, T., Yamane, C., Ueda, K., & Takahashi, K. (2009). Structural reorganization of molecular sheets derived from cellulose II by molecular dynamics simulations. *Carbohydrate Research*, *344*, 1085–1094. https://doi.org/10.1016/j.carres.2009.03.014.

678 Phan, T. N. Q., Le-Vinh, B., Efiana, N. A., & Bernkop-Schnürch, A. (2019). Oral self-
679 emulsifying delivery systems for systemic administration of therapeutic proteins: science
680 fiction? *Journal of Drug Targeting*, *27*, 1017–1024.
681 https://doi.org/10.1080/1061186X.2019.1584200.
682 Pichot, R., Spyropoulos, F., & Norton, I. T. (2010). O/W emulsions stabilised by both low
683 molecular weight surfactants and colloidal particles: The effect of surfactant type and
684 concentration. *Journal of Colloid and Interface Science*, *352*, 128–135.
685 https://doi.org/10.1016/j.jcis.2010.08.021.
686 Premathilaka, R., Rashidinejad, A., Golding, M., & Singh, J. (2022). Oral delivery of
687 hydrophobic flavonoids and their incorporation into functional foods: Opportunities and
688 challenges. *Food Hydrocolloids*, *128*, 107567.
689 https://doi.org/10.1016/j.foodhyd.2022.107567.
690 Product Information. (2020). *Transplantation*, *104*, S13–S16.
691 https://doi.org/10.1097/TP.0000000000003330.
692 Rogerio, A. P., Dora, C. L., Andrade, E. L., Chaves, J. S., Silva, L. F. C., Lemos-Senna, E., &
693 Calixto, J. B. (2010). Anti-inflammatory effect of quercetin-loaded microemulsion in the
694 airways allergic inflammatory model in mice. *Pharmacological Research*, *61*, 288–297.
695 https://doi.org/10.1016/j.phrs.2009.10.005.
696 Sermkaew, N., & Plyduang, T. (2020). Self-microemulsifying drug delivery systems of
697 *Moringa oleifera* extract for enhanced dissolution of kaempferol and quercetin. *Acta*
698 *Pharmaceutica*, *70*, 77–88. https://doi.org/10.2478/acph-2020-0012.
699 Shinoki, A., Lang, W., Thawornkuno, C., Kang, H. K., Kumagai, Y., Okuyama, M., Mori, H.,
700 Kimura, A., Ishizuka, S., & Hara, H. (2013). A novel mechanism for the promotion of
701 quercetin glycoside absorption by megalo α-1,6-glucosaccharide in the rat small intestine.
702 *Food Chemistry*, *136*, 293–296. https://doi.org/10.1016/j.foodchem.2012.08.028.
703 Son, H. Y., Lee, M. S., Chang, E., Kim, S. Y., Kang, B., Ko, H., Kim, I. H., Zhong, Q., Jo, Y.
704 H., Kim, C. T., & Kim, Y. (2019). Formulation and characterization of quercetin-loaded
705 oil in water nanoemulsion and evaluation of hypocholesterolemic activity in rats.
706 *Nutrients*, *11*, 1–19. https://doi.org/10.3390/nu11020244.
707 Sun, G., Zhang, X. Z., & Chu, C. C. (2008). Effect of the molecular weight of polyethylene
708 glycol (PEG) on the properties of chitosan-PEG-poly(*N*-isopropylacrylamide) hydrogels.
709 *Journal of Materials Science: Materials in Medicine*, *19*, 2865–2872.
710 https://doi.org/10.1007/s10856-008-3410-9.
711 Syed, H. K., & Peh, K. K. (2014). Identification of phases of various oil, surfactant/co-

surfactants and water system by ternary phase diagram. *Acta Poloniae Pharmaceutica - Drug Research*, *71*, 301–309.

Thoma, J. A., & French, D. (1960). The starch-iodine-iodide interaction. Part I. spectrophotometric investigations. *Journal of the American Chemical Society*, *82*, 4144–4147. https://doi.org/10.1021/ja01501a004.

Vincken, J. P., De Keizer, A., Beldman, G., & Voragen, A. G. (1995). Fractionation of xyloglucan fragments and their interaction with cellulose. *Plant Physiology*, *108*, 1579–1585. https://doi.org/10.1104/pp.108.4.1579.

Wu, L., Qiao, Y., Wang, L., Guo, J., Wang, G., He, W., Yin, L., & Zhao, J. (2015). A Self-microemulsifying drug delivery system (SMEDDS) for a novel medicative compound against depression: a preparation and bioavailability study in rats. *AAPS PharmSciTech*, *16*, 1051–1058. https://doi.org/10.1208/s12249-014-0280-y.

Xiao, F., Xu, T., Lu, B., & Liu, R. (2020). Guidelines for antioxidant assays for food components. *Food Frontiers*, *1*, 60–69. https://doi.org/10.1002/fft2.10.

Figure captions

Fig. 1. Size characterization of X-MSs prepared by cellulase hydrolysis of tamarind seed xyloglucan. HPAEC-PAD analyses of (A, top) the major saccharides from the original cellulase reaction and (A, bottom) X-MS DP 16 and 56 obtained by methanol purification, and (B) gel filtration HPLC chromatogram of X-MS DP 16 and 56 and the parental xyloglucan. (C) Proposed model structure of X-MS DP 16 and 56 coexisting with the fine structures of XOSs. Subunit names are presented as a one-letter unambiquous nomenclature system as follows: unsubstituted D-Glc*p* is designated **G**, α-D-Xyl*p*-(1→6)-β-D-Glc*p* residue is designated X, β-D-Gal*p*-(1→2)-α-D-Xyl*p*-(1→6)-β-D-Glc*p* is designated **L**, and α-L-Ara*p*-(1→2)-α-D-Xyl*p*-(1→6)-β-D-Glc*p* is designated **A**.

Fig. 2. Fluorescence spectra of TNS (0.5 μM) in the presence of (A) X-MS DP 16 (0–20 mg/mL) and (B) DP 56 (0–10 mg/mL). Inset: the Benesi-Hildebrand double-reciprocal plots for the determination of K_c values of the corresponding X-MSs. Fluorescence intensity at a series concentration of Tween 80 (0.001–0.1 mg/mL) coexisting with (C) X-MS DP 16 (5 and 10 mg/mL) and (D) PEG 550 (10 and 30 mg/mL). Black arrows indicate the direction of the growing concentrations of X-IMSs and PEG. Dashed lines depict the CMC value.

Fig. 3. (A) Ternary phase diagram (by mass fraction) for the mixture of PEG 550, Tween 80, and IPM without quercetin and X-MS. An equal volume of water was added to each fraction. The opened and filled cycles represent the two formulations P0 and P14, respectively, and SMES P0 was categorized as an O/W microemulsion according to Fig. 3B. (B) Variation in microemulsion conductivity at various water contents.

Fig. 4. Effect of MS types and concentrations on the carried dosage of quercetin in the P14 microemulsion. (A) Visual inspection of quercetin loaded into a megalomeric microemulsion of X-MS DP 16, 56, T 3.5, and T 6 with various concentrations after standing overnight (up rows) and then centrifugation at 12,000 ×*g* and 25 °C for 10 min (down rows). The dissolved quercetin in the supernatant of each sample was determined and is presented in (B).

Fig. 5. Droplet analysis of the megalomeric microemulsion. (A) A zetasizer was used to determine the droplet sizes of the microemulsion containing various concentrations of X-MS DP 16 and 56 in the P14 formula. CTRs are the microemulsion template (without quercetin load). The panel compares the sizes of microemulsions containing 3.0% X-MS DP 16 and 56 with and without quercetin loading. (B) The particle appearance of the P0 image obtained by TEM.

Scheme 1. Formulations of megalomeric microemulsions containing quercetin**.**

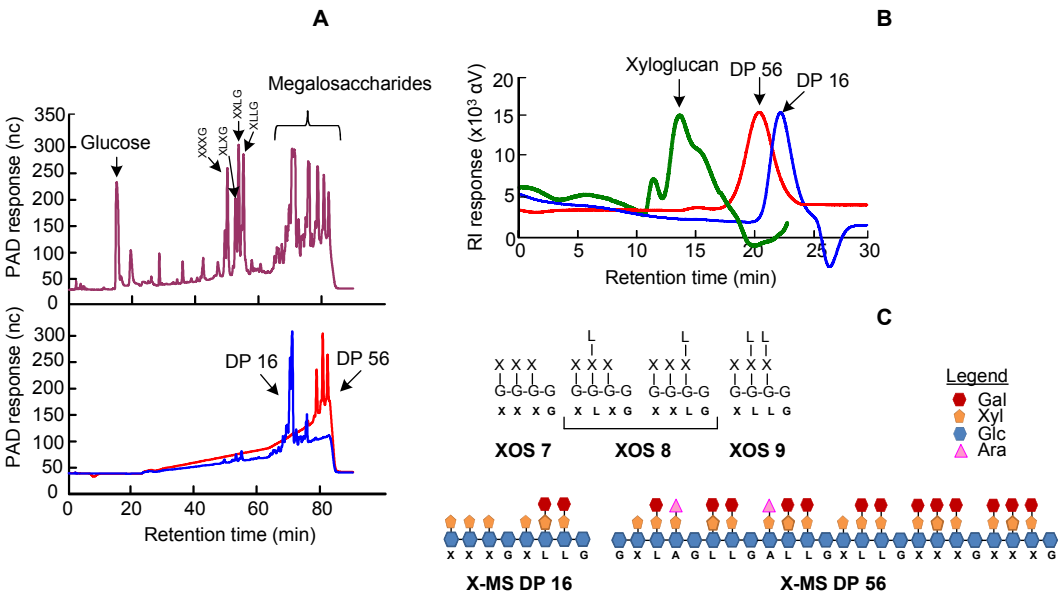

Fig. 1. Size characterization of X-MSs prepared from cellulase hydrolysis.

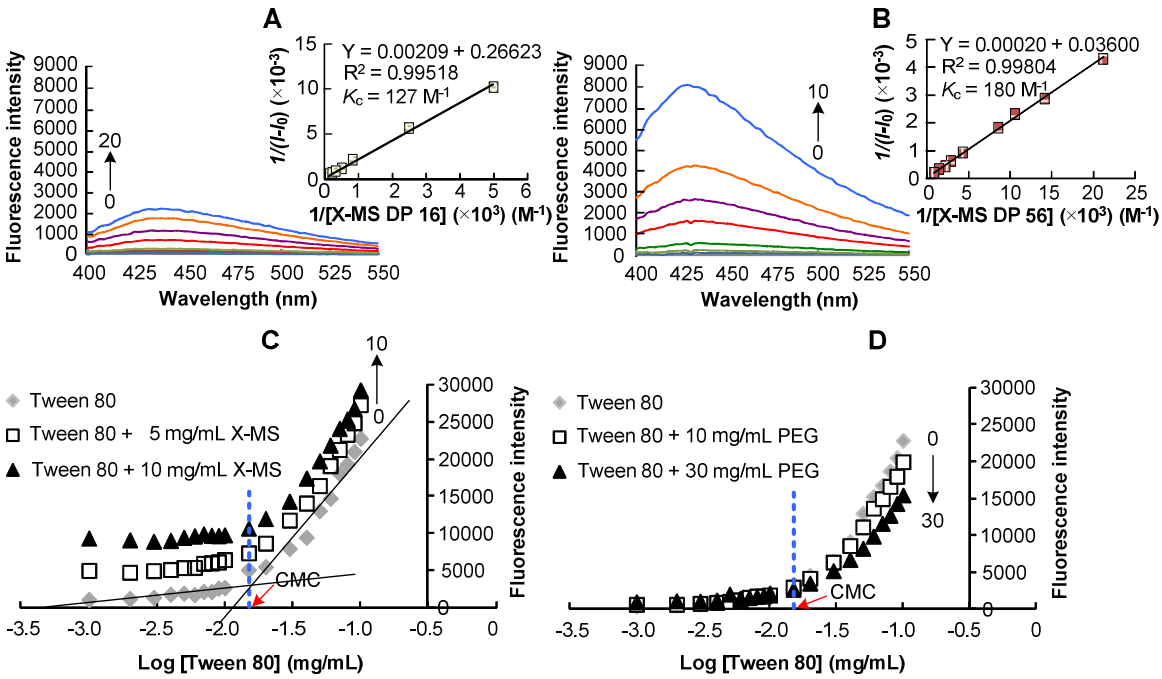

Fig. 2. Fluorescence spectra.

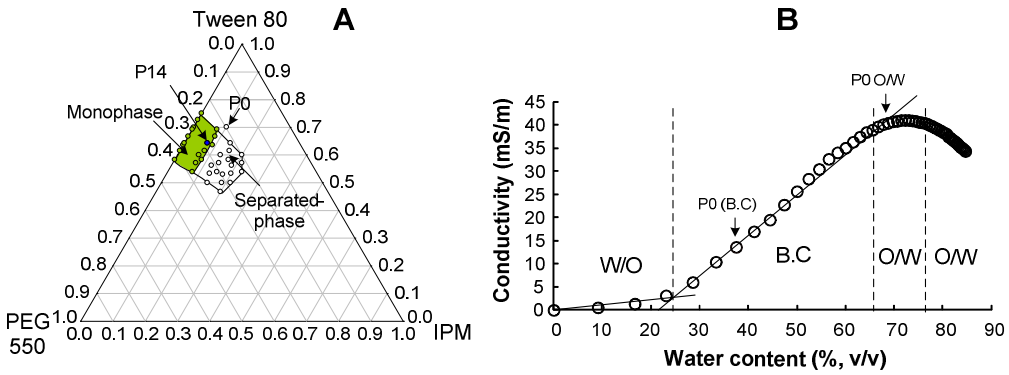

Fig. 3. (A) Ternary phase diagram.

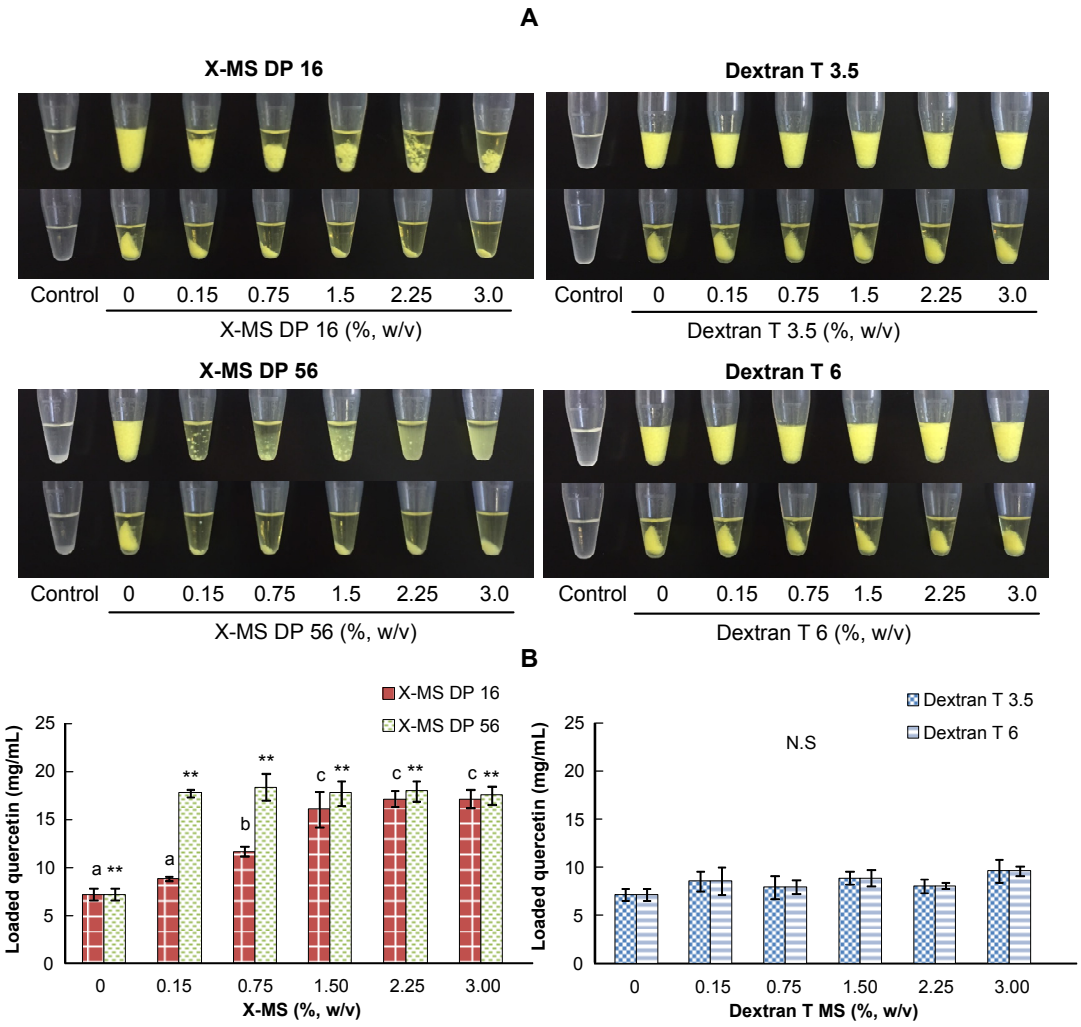

Fig. 4. Effect of MS types.

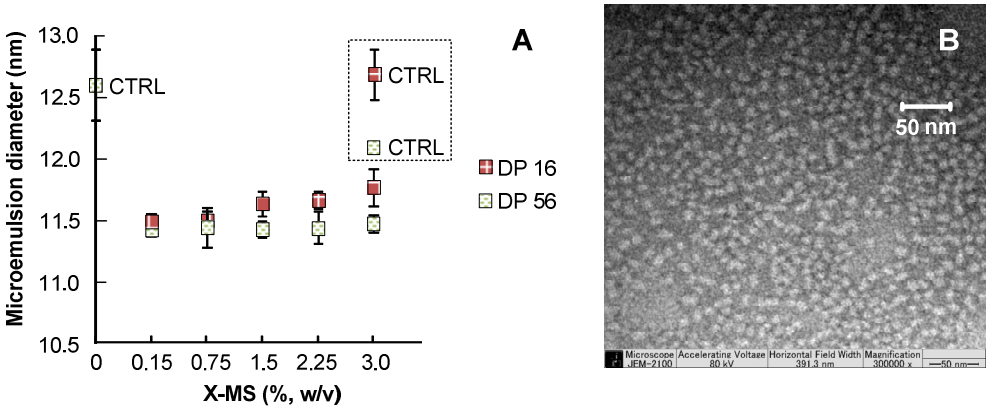

Fig. 5. Droplet analysis of the megalomeric microemulsion.

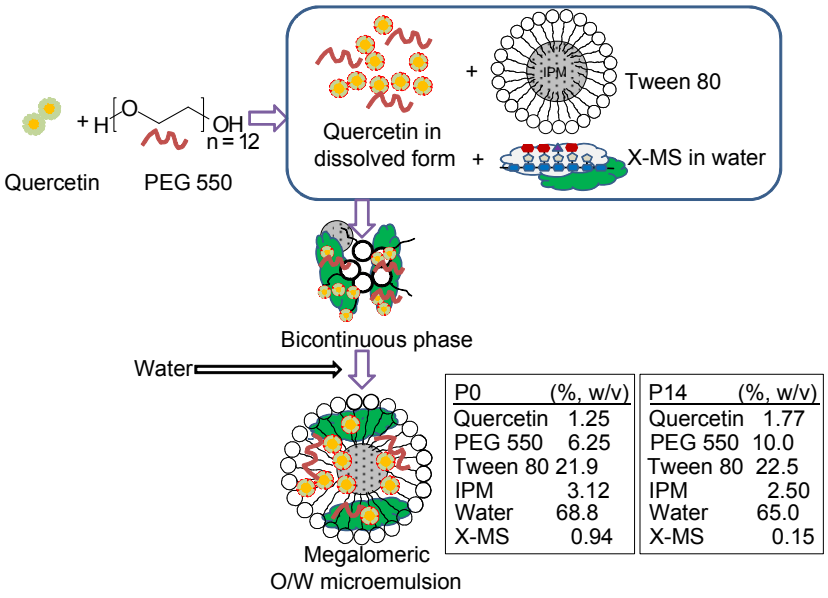

P0	(%, w/v)
Quercetin	1.25
PEG 550	6.25
Tween 80	21.9
IPM	3.12
Water	68.8
X-MS	0.94

P14	(%, w/v)
Quercetin	1.77
PEG 550	10.0
Tween 80	22.5
IPM	2.50
Water	65.0
X-MS	0.15

Scheme 1. Formulations of the megalomeric microemulsion**.**

Table 1. Phase solubility of quercetin in fixed-dose excipients with or without the addition of X-MS DP 56 or Tween 80.

Excipient	Quercetin solubility (mg/mL)			
	no water	with water[a]	with X-MS and water[b]	with Tween 80 and water[c]
PEG 200	204.57 ± 1.37	0.08 ± 0.01	0.82 ± 0.02	2.17 ± 0.10
PEG 300	201.86 ± 1.37	0.10 ± 0.00	0.74 ± 0.04	2.36 ± 0.12
PEG 400	196.62 ± 0.55	0.12 ± 0.00	1.09 ± 0.03	2.48 ± 0.01
PEG 550	203.80 ± 1.37	0.16 ± 0.01	1.38 ±0.25	2.51 ± 0.03
PEG 1000	N.D	0.05 ± 0.00	0.31 ± 0.01	1.33 ± 0.04
PEG 4000	N.D	0.08 ± 0.00	0.26 ± 0.01	1.14 ± 0.00
PEG 6000	N.D.	0.07 ± 0.00	0.21 ± 0.00	1.18 ± 0.10
PEG 8000	N.D.	0.07 ± 0.01	0.20 ± 0.00	0.94 ± 0.01
Glycerol	2.60 ± 0.12	0.01 ± 0.00	0.15 ± 0.00	1.81 ± 0.41
Tween 80	6.30 ± 0.14	1.63 ± 0.04	1.83 ± 0.13	

N.D. = not determined because the original forms are semisolid or solid. [a] The combination contains 20% PEG in water. [b] The combination contains 10%, (w/v) X-MS and 20% PEG and replenished with water to be 100% (v/v). [c] The combination contains 10% (v/v) Tween 80 and 20% PEG or 10% (v/v) glycerol.

Table 2. Maximum quercetin load in the P0 microemulsion containing saccharides.

Saccharides	Quercetin solubility (mg/mL)	Precipitant found
-[a]	0.11 ± 0.15	+++
-[b]	6.80 ± 0.50	+++
Maltoheptaose	8.37 ± 0.15	++
α-CD	8.32 ± 1.43	+++
β-CD	6.02 ± 0.70	+++
γ-CD	7.39 ± 0.68	+++
XOS 9	11.57 ± 0.16	+
X-MS DP 16	12.04 ± 0.07	-/+
X-MX DP 56	12.50 ± 0.20	-
Soluble starch	11.53 ± 0.05	+
Gum arabic	10.57 ± 0.66	+
Dextran T 40	8.97 ± 0.49	++

[a] = Dissolved quercetin with PEG 550 and then loaded into water, [b] = Dissolved quercetin with PEG 550 and then loaded into P0 using water instead of saccharides. - = no precipitate, +, ++, +++ = small, moderate, and complete precipitate, respectively.

954 **Table 3.** IC50 (μg/mL) determination by DPPH and ABTS assays.

	DPPH		ABTS
Quercetin in	at pH 6.0	at pH 7.4	at pH 4.0
Methanol	38.0 ± 10	176.9 ± 10.0	48.3 ± 2.5
Microemulsion without X-MS	89.7 ± 0.3	125.1 ± 9.8	49.8 ± 2.8
Microemulsion with X-MS DP 16	22.2 ± 1.6	111.2 ± 9.8	48.8 ± 8.0
Microemulsion with X-MS DP 56	24.1 ± 1.2	122.7 ± 9.6	48.7 ± 11.0

955